

## Supporting Information

### Band Structure Engineering of the W Replacement in ReSe<sub>2</sub>

#### Nanosheets for Enhancing Hydrogen Evolution

Xiaowei Guo,<sup>†ab</sup> Tong Wu,<sup>†ab</sup> Siwei Zhao,<sup>†c</sup> Yuqiang Fang,<sup>a</sup> Shumao Xu,<sup>a</sup> Miao Xie<sup>ab</sup>  
and Fuqiang Huang<sup>\*ac</sup>

<sup>a</sup>State Key Laboratory of High Performance Ceramics and Superfine Microstructure, Shanghai Institute of Ceramics, Chinese Academy of Sciences, Shanghai 200050, P. R. China

<sup>b</sup>University of Chinese Academy of Sciences, Beijing 100049, China

<sup>c</sup>State Key Laboratory of Rare Earth Materials Chemistry and Applications, College of Chemistry and Molecular Engineering, Peking University, Beijing 100871, P.R. China

#### AUTHOR INFORMATION

E-mail: huangfq@mail.sic.ac.cn

## Experimental Section

### Material Preparation

The bulk  $\text{Re}_{1-x}\text{W}_x\text{Se}_2$  ( $0 \leq x \leq 0.3$ ) crystals were synthesized via high temperature solid-state reaction. Re powder, W powder and Se powder were mixed according to stoichiometric ratio and pressed into a pellet. It was transferred into muffle furnace and annealed at 1323 K for 24 hours with the heating rate of  $5 \text{ K} \cdot \text{min}^{-1}$ . Afterwards, the samples were cooled down to room temperature naturally. Ultimately, the samples were dispersed in deionized water and dried in a vacuum oven at room temperature.  $\text{Re}_{1-x}\text{W}_x\text{Se}_2$  nanosheets were obtained from an ultrasonication-assisted exfoliation process. In a typical procedure, 0.5 g of bulk  $\text{Re}_{1-x}\text{W}_x\text{Se}_2$  powder was added to 30 mL of N,N-dimethylformamide (DMF) in a 50 mL glass vial and this mixture was subjected to ultrasonication for 24 h to get the exfoliated  $\text{Re}_{1-x}\text{W}_x\text{Se}_2$  NSs.

### Materials characterization

X-ray diffraction (XRD) characterization was carried out by Bruker D8 advance. Raman spectra were obtained using a thermal dispersive spectrometer with laser excitation at 635nm. Material microstructure was observed by a Hitachi S-4800 field emission scanning electron microscope (SEM). Transmission Electron Microscopy (TEM) images were obtained by JEOL JEM-2100F. X-ray Photoelectron Spectroscopy (XPS) measurements were run on a Thermo VG Scientific with Al  $K\alpha$  radiation ( $\lambda = 1486.6 \text{ eV}$ ). The images were imaged in high Angle annular dark field (HAADF) and bright field (BF), obtaining the mass-thickness and diffraction contrast information, respectively. The internal and external receiving angles of HAADF imaging were 68 and 280 m rad, respectively, and the receiving angles of BF imaging were 17 m rad.

### Electrochemical measurements

The electrochemical experiment was carried out using a CHI-760E electrochemical workstation at ambient temperature. The measurements were performed in 0.5 M  $\text{H}_2\text{SO}_4$  solution (deaerated by Ar) using a three-electrode setup, with a saturated calomel electrode (in saturated KCl solution) reference electrode, a graphite rod counter electrode and the glassy carbon working electrode. The catalyst was treated by ultrasonically dispersing in

Nafion/alcohol solution (0.5 wt.%, Alfa Aesar) to obtain  $5.0 \text{ mg mL}^{-1}$  slurry. The catalyst was dispersed in Nafion/alcohol solution (0.5 wt.%, Alfa Aesar) by sonication for 60 min. Then,  $10 \text{ }\mu\text{L}$  of the mixed solution was drop-casted onto a glassy carbon rotating disk working electrode (5 mm diameter) and dried with  $\text{N}_2$ . Initially, cyclic voltammogram (CV) was operated at least 20 cycles to guarantee the activation of the catalyst. LSV scan rate was  $0.01 \text{ V}\cdot\text{s}^{-1}$ . The electrochemical active surface area (ECSA) of the catalyst was tested in this way, that double-layer capacitance ( $C_{dl}$ ) was tested in the potential window of  $-0.25 \sim -0.15 \text{ V}$  (vs. RHE) at the scan rates of 20, 40, 60, 80, 100 and  $120 \text{ mV}\cdot\text{s}^{-1}$  in the CV model.

### **Theoretical calculation**

The calculations were based on the density functional theory (DFT) using Vienna Ab-initio Simulation Package (VASP). Ultra-soft (US) pseudopotentials and Perdew-Burke-Ernzerhof (PBE) parameterization of the generalized gradient approximation (GGA) are applied for the core-valence electron interaction and exchange-correlation functional, respectively. The cutoff energy was set as 600 eV. The total energy convergence was less than  $10^{-4} \text{ eV}$  per atom. The force-on-atom was converged below a threshold of 0.02. For  $\text{WS}_2$  or  $\text{ReSe}_2$ , a  $12 \times 12 \times 3$  or  $6 \times 6 \times 6$  Monkhorst-Pack K-point grid was applied based on single cell unit for density of states (DOS). For  $\text{Re}_{0.7}\text{W}_{0.3}\text{Se}_2$ , one Re atom was substituted by W in  $\text{ReSe}_2$ .

## Supporting Figures

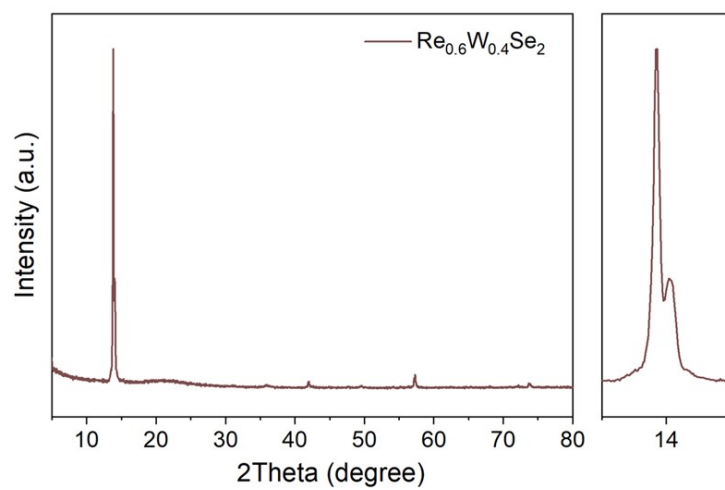


**Figure S1.** Powder X-ray diffraction pattern of  $\text{Re}_{0.6}\text{W}_{0.4}\text{Se}_2$  is calculated by stoichiometry.

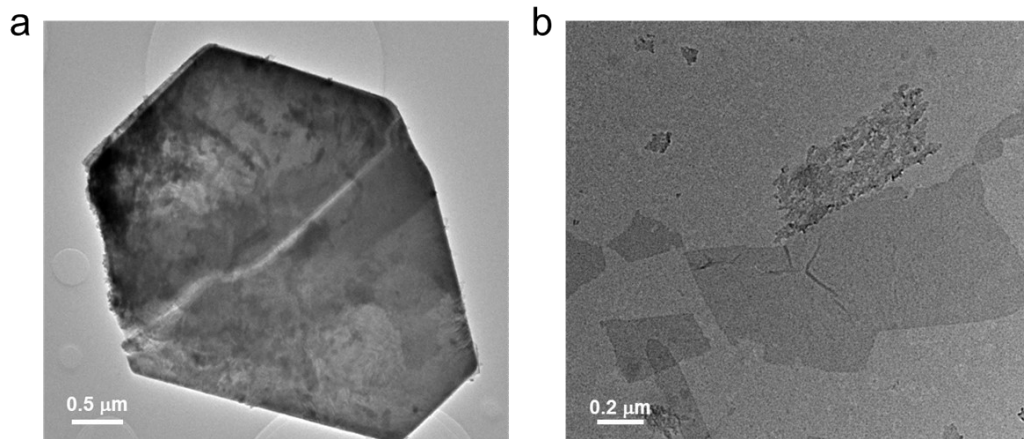


**Figure S2.** SEM images of (a) bulk  $\text{Re}_{0.7}\text{W}_{0.3}\text{Se}_2$  and (b)  $\text{Re}_{0.7}\text{W}_{0.3}\text{Se}_2$  nanosheets.

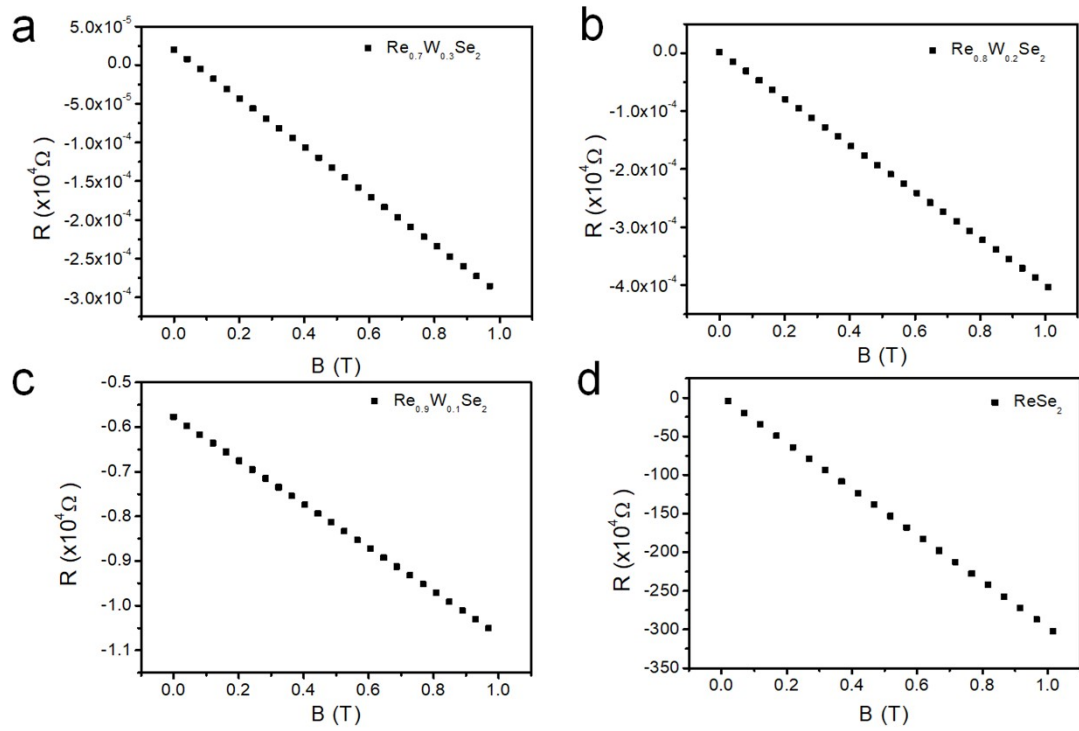


**Figure S3.** Room-temperature Hall measurements based on  $\text{Re}_{1-x}\text{W}_x\text{Se}_2$  crystals. Typical plot of the transverse Hall resistance  $R$  versus an external magnetic field ( $B$ ) for the  $\text{Re}_{1-x}\text{W}_x\text{Se}_2$  ( $x = 0.3, 0.2, 0.1$  and 0) crystals.

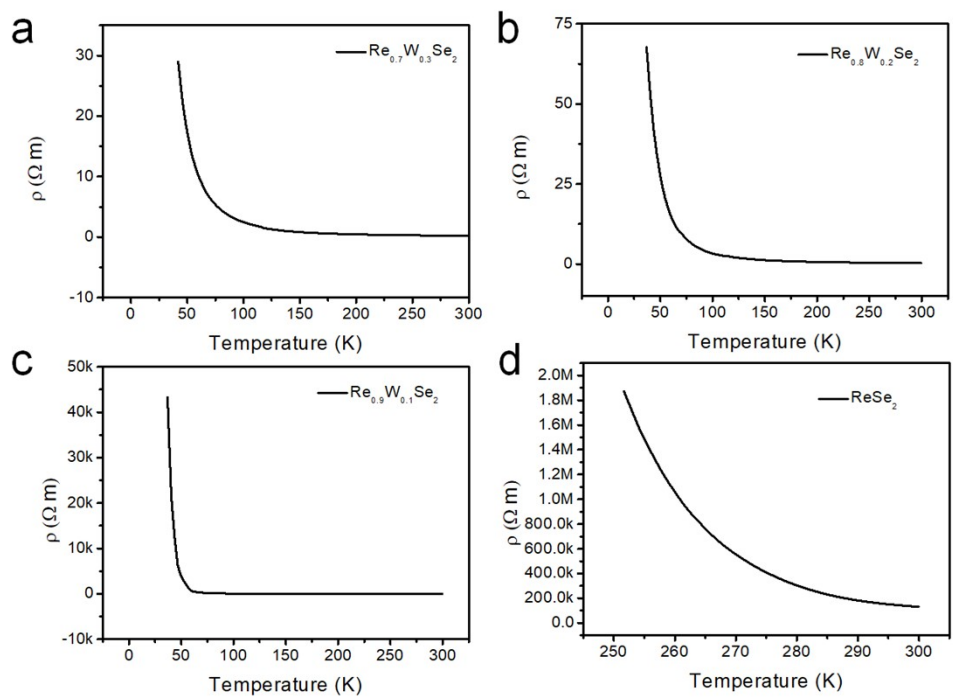


**Figure S4.** The temperature-dependent resistivity (R-T) curves of  $\text{Re}_{0.7}\text{W}_{0.3}\text{Se}_2$ ,  $\text{Re}_{0.8}\text{W}_{0.2}\text{Se}_2$ ,  $\text{Re}_{0.9}\text{W}_{0.1}\text{Se}_2$  and  $\text{ReSe}_2$ .

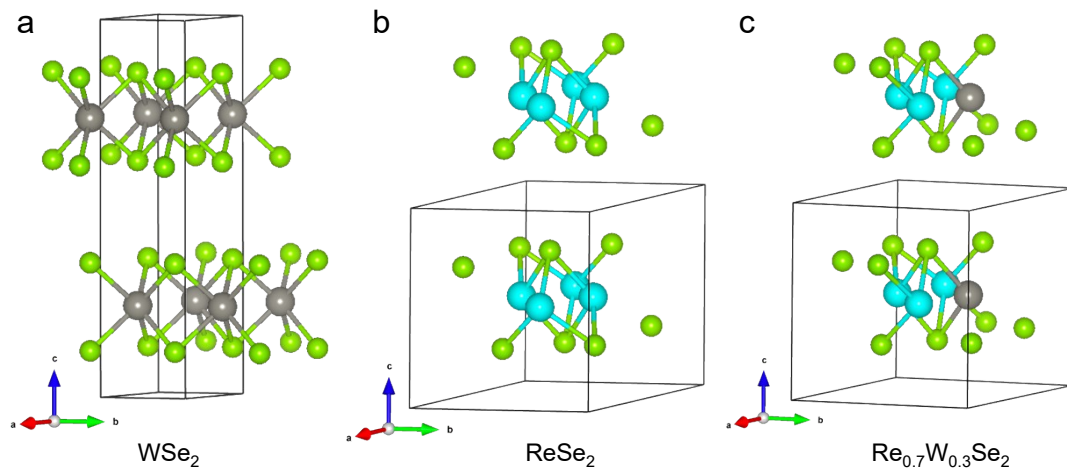


**Figure S5.** Geometrically optimized cells of  $\text{WSe}_2$  (a),  $\text{ReSe}_2$  (b) and W-doped  $\text{ReSe}_2$  (c).



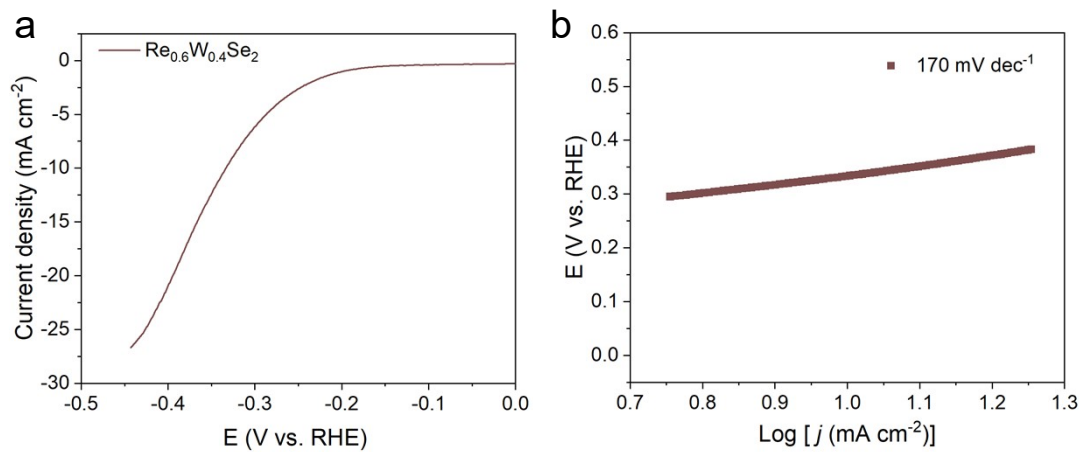


**Figure S6.** (a) Linear sweep voltammetry (LSV) curves of  $\text{Re}_{0.6}\text{W}_{0.4}\text{Se}_2$ . (b) Tafel plots derived from the LSV curves.

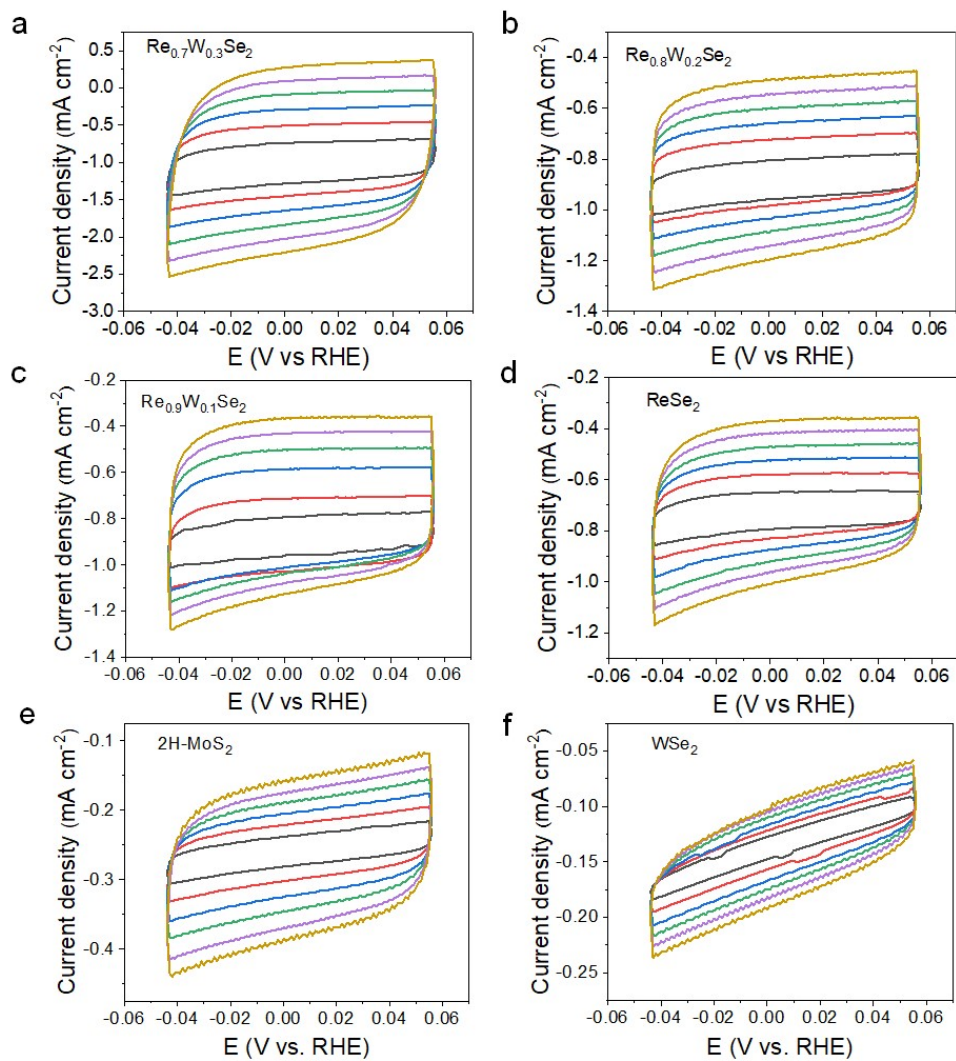


**Figure S7.** Cyclic voltammograms (CVs) of as-prepared samples: (a)  $\text{Re}_{0.7}\text{W}_{0.3}\text{Se}_2$ , (b)  $\text{Re}_{0.8}\text{W}_{0.2}\text{Se}_2$ , (c)  $\text{Re}_{0.9}\text{W}_{0.1}\text{Se}_2$ , (d)  $\text{ReSe}_2$ , (e)  $2\text{H-MoS}_2$  and (f)  $\text{WSe}_2$ . Current density is the difference between anodic and cathodic current densities at 0.06 V (*vs* RHE). In the plot, the capacitance was normalized by the geometric surface area of electrodes.

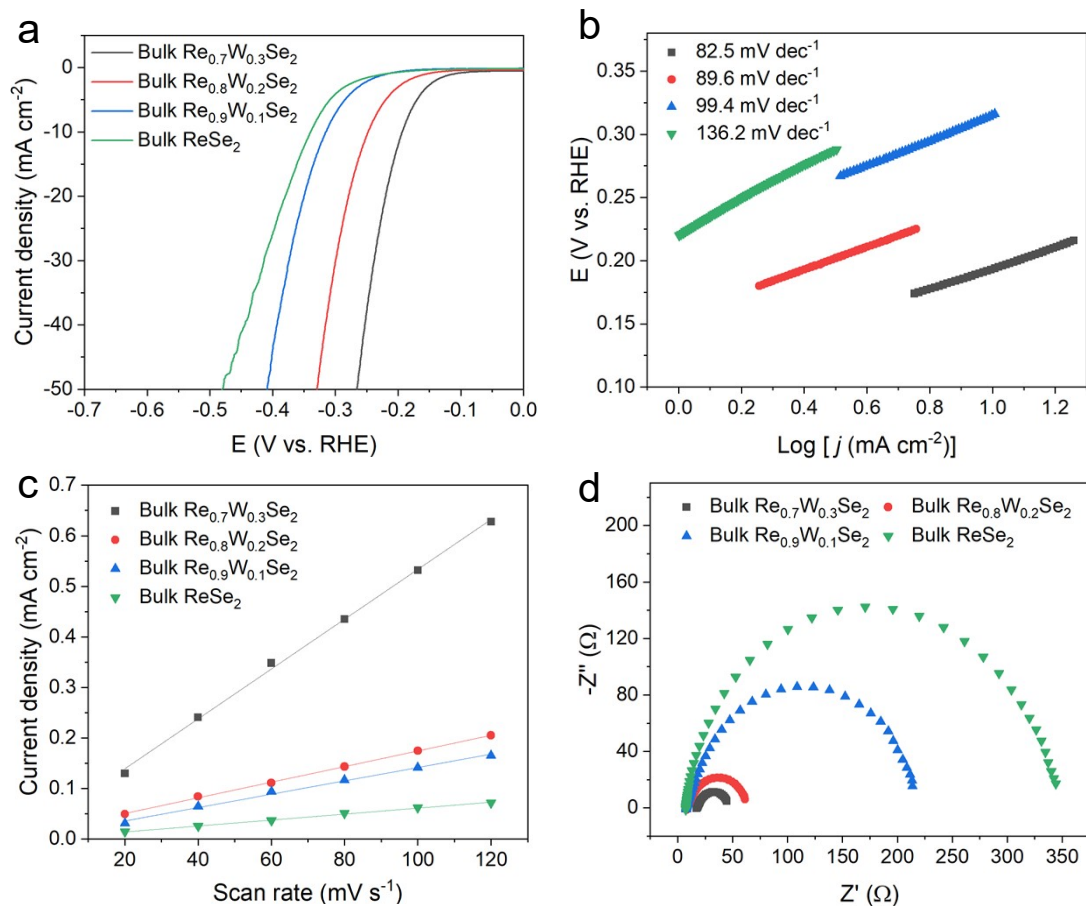


**Figure S8.** HER performance in 0.5M  $\text{H}_2\text{SO}_4$ . (a) Linear sweep voltammetry (LSV) curves of bulk  $\text{Re}_{1-x}\text{W}_x\text{Se}_2$ . (b) Tafel plots derived from the LSV curves. (c) ECSA at  $E=0.06$  V versus RHE (reversible hydrogen electrode) for  $\text{Re}_{1-x}\text{W}_x\text{Se}_2$ . (d) Electrochemical impedance spectroscopy Nyquist plots of  $\text{Re}_{1-x}\text{W}_x\text{Se}_2$  samples.

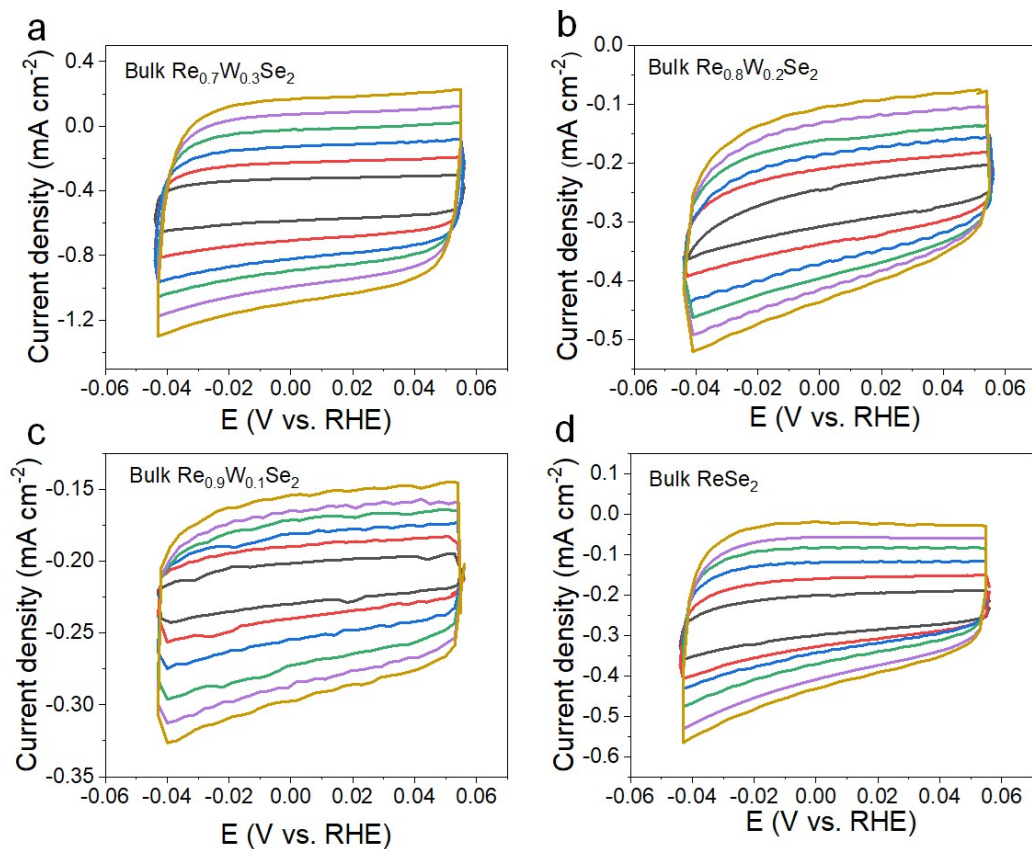


**Figure S9.** Cyclic voltammograms (CVs) of as-prepared samples: (a) bulk  $\text{Re}_{0.7}\text{W}_{0.3}\text{Se}_2$ , (b) bulk  $\text{Re}_{0.8}\text{W}_{0.2}\text{Se}_2$ , (c) bulk  $\text{Re}_{0.9}\text{W}_{0.1}\text{Se}_2$  and (d) bulk  $\text{ReSe}_2$ . Current density is the difference between anodic and cathodic current densities at 0.06 V (vs RHE). In the plot, the capacitance was normalized by the geometric surface area of electrodes.

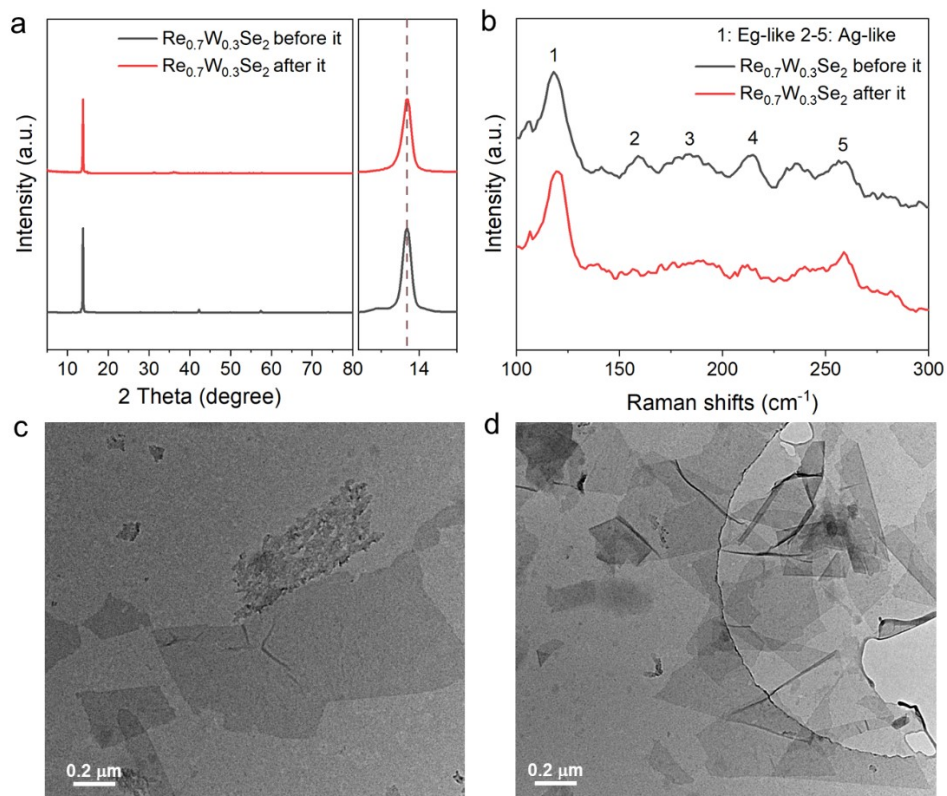


**Figure S10.** (a) XRD patterns and (b) Raman spectra of  $\text{Re}_{0.7}\text{W}_{0.3}\text{Se}_2$  before and after long-term HER test. (c-d) Comparison of morphology before and after long-term HER test.

## Cell parameter

**Table S1.** Comparison of cell parameters between calculated WSe<sub>2</sub>, ReSe<sub>2</sub> and W-doped ReSe<sub>2</sub>.

Parameters	WSe <sub>2</sub>	ReSe <sub>2</sub>	Re <sub>0.7</sub> W <sub>0.3</sub> Se <sub>2</sub>
<i>a</i> (Å)	3.30694	6.65953	6.53146
<i>b</i> (Å)	3.30694	6.78769	6.81014
<i>c</i> (Å)	14.47976	7.51733	7.59956
$\alpha$ (°)	90.0000	91.9787	93.0375
$\beta$ (°)	90.0000	103.6890	102.9353
$\gamma$ (°)	120.0000	118.8190	118.4648